

Advance Publication Cover Page



**2-Aminoethanesulfonic acid immobilized on epichlorohydrin functionalized  
 $\text{Fe}_3\text{O}_4@ \text{WO}_3$  ( $\text{Fe}_3\text{O}_4@ \text{WO}_3\text{-EAE-SO}_3\text{H}$ ): a novel magnetically recyclable  
heterogeneous nanocatalyst for the green one-pot synthesis of  
1-substituted-1*H*-1,2,3,4-tetrazoles in water**

Maryam Sadat Ghasemzadeh and Batool Akhlaghinia\*

Advance Publication on the web July 31, 2017

doi:10.1246/bcsj.20170148

© 2017 The Chemical Society of Japan

# 2-Aminoethanesulfonic acid immobilized on epichlorohydrin functionalized $\text{Fe}_3\text{O}_4@ \text{WO}_3$ ( $\text{Fe}_3\text{O}_4@ \text{WO}_3\text{-EAE-SO}_3\text{H}$ ): a novel magnetically recyclable heterogeneous nanocatalyst for the green one-pot synthesis of 1-substituted-1*H*-1,2,3,4-tetrazoles in water

Maryam Sadat Ghasemzadeh and Batool Akhlaghinia\*

Department of Chemistry, Faculty of Sciences, Ferdowsi University of Mashhad, 9177948974 Mashhad, Iran

E-mail: akhlaghinia@um.ac.ir

## Abstract

In this research 2-aminoethanesulfonic acid immobilized on epichlorohydrin functionalized  $\text{Fe}_3\text{O}_4@ \text{WO}_3$  ( $\text{Fe}_3\text{O}_4@ \text{WO}_3\text{-EAE-SO}_3\text{H}$ ) has been introduced as a novel and efficient magnetic nanocatalyst for appropriate and rapid synthesis of 1-substituted-1*H*-1,2,3,4-tetrazoles. This new nanocatalyst was then characterized using FT-IR, XRD, TEM, EDS, TGA, FE-SEM, CHNS and VSM techniques. The above experimental results determined the composition of  $\text{Fe}_3\text{O}_4@ \text{WO}_3\text{-EAE-SO}_3\text{H}$  and clearly revealed that the nanoparticles are spherical in shape with the particle size in the range of 7–23 nm and superparamagnetic behavior.  $\text{Fe}_3\text{O}_4@ \text{WO}_3\text{-EAE-SO}_3\text{H}$  as an excellent instance to replace Brønsted acids was shown to be highly efficient in the rapid preparation of 1-substituted-1*H*-1,2,3,4-tetrazoles through the cyclization reaction of various primary amines, triethyl orthoformate and 1-butyl-3-methylimidazolium azide ([bmim][N<sub>3</sub>]). Compared with conventional methods, the present protocol has the considerable advantages such as short reaction time, mild reaction conditions, easy work-up, pure products with high yields, recovering the catalyst using an external magnet and reusing the catalyst several times without noticeable deterioration in catalytic activity. In addition to the aforementioned favorable properties, the remarkable feature of the present protocol is the use of water as environmentally benign solvent, which eliminates the use of toxic solvent.

## 1. Introduction

Nitrogen-containing compounds have always remained a major source for therapeutic drugs and have received significant attention.<sup>1</sup> Among them nitrogen-containing heterocycles such as tetrazoles have attracted considerable interest because of their wide range of applications in material sciences (including explosives and rocket propellants), synthetic organic chemistry as analytical reagents,<sup>2</sup> and synthons for a variety of nitrogen containing heterocycles.<sup>3-9</sup> Tetrazoles have been successfully used in coordination chemistry as ligands for many useful transformations<sup>10,11</sup> and in medicinal chemistry as a surrogate for carboxylic acid functionalities which exhibit favourable pharmacokinetic profit and metabolic stability.<sup>12</sup>

Furthermore, tetrazoles played main roles in information recording systems and photography.<sup>13-24</sup> Recently, because of the effective usefulness of this heterocyclic nucleus, the synthesis of tetrazole frameworks is of much current importance, and various preparative methods have been developed. 1-Substituted-1*H*-1,2,3,4-tetrazoles as a special category of tetrazoles have been reported since the last mid-century and only a few methods for synthesis of this compounds have been reported.<sup>14,17</sup> One of the main routes for the synthesis of 1-substituted-1*H*-1,2,3,4-tetrazoles, involves acid-catalyzed cycloaddition between isocyanides and hydrazoic acid or, trimethylsilyl azide.<sup>25-27</sup> This method often includes a number of steps and is insufficiently effective. Another method (as the most promising method) of 1-substituted-1*H*-1,2,3,4-tetrazoles synthesis is based on the reaction of amines with ethyl orthoformate or orthocarboxylic acid ester and sodium azide in the presence of acetic acid, trifluoroacetic acid,  $\text{PCl}_5$ , ionic liquid and DMSO and ytterbium triflate in highly polar solvents.<sup>28-35</sup> Unfortunately, some of the earlier reported methods for the synthesis of 1-substituted-1*H*-1,2,3,4-tetrazoles have one or more of the following drawbacks such as harsh reaction conditions (the presence of excess amounts of hydrazoic acid, which is highly toxic, explosive and volatile), expensive and toxic metal catalysts and reagents, difficulty in obtaining and/or preparing the starting materials, high boiling solvents, refluxing for a prolonged period of time, low yield and tedious work-up. As the lack of convenient methods for the preparation of 1-substituted tetrazoles should not restrict their potential applications, a continuing interest for the formation of this class of heterocyclic compounds is still challenging and demand at the forefront of synthetic organic chemistry. In last decade, magnetic nanoparticles have received a remarkable attention due to their unique physicochemical properties and potential applications in numerous areas.<sup>36</sup> Iron oxides and other iron-containing nanoparticles are the most widely studied magnetic nanomaterials.<sup>37</sup> To control the size, shape, stability and dispersibility of the magnetic nanomaterials (as a technological challenge) they have been coated with organic or inorganic protective layers (to avoid the

aggregation/oxidation and serves as the catalyst platform) such as polymer,<sup>38</sup> silica,<sup>39</sup> zeolite,<sup>40</sup> carbon,<sup>41</sup> hydroxyapatite<sup>42</sup> and metal oxides.<sup>43</sup> Tungsten is one of the most important economical and environmentally well-suited metal in our globe.<sup>44</sup> Interest in tungsten oxides ( $\text{WO}_x$ ) can be dated back to the 17th century.<sup>45</sup> Tungsten trioxide ( $\text{WO}_3$ ) with wide range of applications in everyday life and in several research fields (from condensed matter physics to solid-state chemistry) is commercially available.<sup>44</sup> As nanostructured  $\text{WO}_3$  is exceptionally versatile and offers unique characteristics, the synthesis and analysis of  $\text{WO}_3$  nanostructures have become increasingly prominent. So far, different heterogeneous catalysts based on  $\text{WO}_3$  nanoparticles have been reported in some organic reactions such as oxidation of primary amines to oximes using  $\text{WO}_3/\text{Al}_2\text{O}_3$ ,<sup>46</sup> oxidation of olefins, sulfides and cyclic ketones by  $\text{WO}_3$  /MCM-48,<sup>47</sup> synthesis of 1,8-dioxo-octahydroxanthene, tetrahydrobenzoxanthene and benzimidazolo quinazolinone derivatives in the presence of  $\text{WO}_3\text{-SO}_3\text{H}$  (WSA),<sup>44</sup> synthesis of alkyl levulinates from levulinic acid using  $\text{WO}_3\text{-SBA-16}$ ,<sup>48</sup> preparation of  $\text{WO}_3$ @PdO core-shell nanospheres as a reusable catalyst in Mizoroki–Heck reaction<sup>49</sup> and synthesis of  $\text{Fe}_3\text{O}_4/\text{WO}_3$  as a high-performance and recyclable visible-light photocatalyst.<sup>50</sup> In continuing of our interests in developing new heterogeneous catalysts<sup>51-64</sup> in organic transformations, herein we wish to design 2-aminoethanesulfonic acid immobilized on epichlorohydrin functionalized  $\text{Fe}_3\text{O}_4$ @ $\text{WO}_3$  ( $\text{Fe}_3\text{O}_4$ @ $\text{WO}_3\text{-EAE-SO}_3\text{H}$ ), as a novel and magnetically recyclable heterogeneous acidic catalyst (Scheme 1). The  $\text{Fe}_3\text{O}_4$  MNPs were prepared by the method described in the literature<sup>65</sup> which consists of coprecipitation of Fe(III) and Fe(II) in alkaline solution. Given the aforementioned advantages of  $\text{WO}_3$ ,  $\text{Fe}_3\text{O}_4$  MNPs were then coated by  $\text{WO}_3$  shell through the reaction with  $\text{WCl}_6$  and subsequent oxidation which leads to formation of  $\text{Fe}_3\text{O}_4$ @ $\text{WO}_3$  (**I**). Suspension of **I** in pure epichlorohydrin at 60 °C with vigorous stirring results epichlorohydrin functionalized  $\text{Fe}_3\text{O}_4$ @ $\text{WO}_3$  ( $\text{Fe}_3\text{O}_4$ @ $\text{WO}_3\text{-E}$ ) (**II**). Afterwards,  $\text{Fe}_3\text{O}_4$ @ $\text{WO}_3\text{-EAE-SO}_3\text{H}$  (**III**) was obtained by treating of **II** with 2-aminoethanesulfonic acid (taurine) as a bifunctional organic molecule that has both  $-\text{SO}_3\text{H}$  and  $-\text{NH}_2$  groups. It can be used as a surface modification agent. 2-Aminoethanesulfonic acid (taurine) as a "conditionally essential" amino acid was found throughout the body particularly in the brain, eyes, heart and muscles.<sup>66</sup> Body can produce some amount of taurine, and it is also found in some foods such as meat, fish and dairy.<sup>67</sup>

## 2. Experimental

**2.1 General.** All chemical reagents and solvents were purchased from Merck and Sigma-Aldrich chemical

companies and were used as received without further purification. The purity determinations of the products were accomplished by TLC on silica gel polygram STL G/UV 254 plates. The melting points of the products were determined with an Electrothermal Type 9100 melting point apparatus. The FT-IR spectra were recorded on an Avatar 370 FT-IR Thermo Nicolet spectrometer. Elemental analyses were performed using a Thermo Finnegan Flash EA 1112 Series instrument. The NMR spectra were obtained in Bruker Avance 300 MHz instruments in  $\text{CDCl}_3$  or  $\text{DMSO-}d_6$ . Mass spectra were recorded with a CH7A Varianmat Bremem instrument at 70 eV electron impact ionization, in  $m/z$  (rel %). TGA analysis was carried out on a Shimadzu Thermogravimetric Analyzer (TG-50) in the temperature range of 25–600 °C at a heating rate of 10 °C  $\text{min}^{-1}$  under air atmosphere. Transmission electron microscopy (TEM) was performed with a Leo 912 AB microscope (Zeiss, Germany) with an accelerating voltage of 120 kV. Elemental compositions were determined with a Leo 1450 VP scanning electron microscope equipped with an SC7620 energy dispersive spectrometer (SEM-EDS) presenting a 133 eV resolution at 20 kV. FE-SEM images were recorded using a TESCAN, Model: MIRA3 scanning electron microscope operating at an acceleration voltage of 30.0 kV and resolution of about 200 and 500 nm (manufactured by Czech Republic). The crystal structure of catalyst was analyzed by XRD using Model Explorer Company: GNR (Italy) diffractometer Dectvis operated at 40 kV and 30 mA utilizing Cu  $K\alpha$  radiation ( $\lambda=0.154 \text{ \AA}$ ). The magnetic property of catalyst was measured using a vibrating sample magnetometer (VSM, Magnetic Danesh Pajoh Inst.). All yields refer to isolated products after purification by recrystallization.

**2.2 Preparation of Magnetite Nanoparticles ( $\text{Fe}_3\text{O}_4$  NPs).**  $\text{FeCl}_2\cdot 4\text{H}_2\text{O}$  (10mmol, 1.99 g) and  $\text{FeCl}_3\cdot 6\text{H}_2\text{O}$  (12mmol, 3.25 g) were dissolved in deionized water (30 mL) under  $\text{N}_2$  atmosphere at room temperature.  $\text{NH}_4\text{OH}$  solution (0.6 M, 200 mL) was then added drop wise to the stirring mixture at room temperature to reach the reaction pH to 11. The resulting black dispersion was continuously stirred for 1 h at room temperature, and heated to reflux for 1 h to yield a brown dispersion. The magnetic nanoparticles were subsequently separated by a magnetic bar and washed with deionized water until it was neutralized.  $\text{Fe}_3\text{O}_4$  NPs was then dried at ambient temperature for 24 h.

**2.3 Preparation of  $\text{Fe}_3\text{O}_4$ @ $\text{WO}_3$  core-shell (**I**).**<sup>50</sup>  $\text{WCl}_6$  (0.5mmol, 0.198 g), ethylene glycol (20 mL) and  $\text{Fe}_3\text{O}_4$  magnetic nanoparticle (1.5mmol, 0.346g) were added to absolute ethanol (80 mL) under mild stirring. The resulting black suspension was loaded into a Teflon-lined autoclave, which was then sealed, heated to 180°C for 24 h, and then allowed to cool to room temperature. The final product was rinsed by absolute ethanol, and then dried at

70 °C for 1 h. Afterwards the resulting  $\text{Fe}_3\text{O}_4/\text{W}_{18}\text{O}_{49}$  precursor was heated at 420 °C for 6 h to produce  $\text{Fe}_3\text{O}_4@/\text{WO}_3$  (I).

**2.4 Preparation of epichlorohydrin functionalized  $\text{Fe}_3\text{O}_4@/\text{WO}_3$  ( $\text{Fe}_3\text{O}_4@/\text{WO}_3\text{-E}$ ) (II).**  $\text{Fe}_3\text{O}_4@/\text{WO}_3$  (0.7 g) was dispersed in 6 mL pure epichlorohydrin by sonication for 30 min. The resultant suspension was heated at 60 °C with vigorous stirring. After 24 h the epichlorohydrin-functionalized  $\text{Fe}_3\text{O}_4@/\text{WO}_3$  was separated by an external magnet and washed with MeOH (5 × 10 mL) until removing additional amount of epichlorohydrine. Then  $\text{Fe}_3\text{O}_4@/\text{WO}_3\text{-E}$  (II) was dried at 40 °C under vacuum for 14 h.

**2.5 Preparation of 2-aminoethanesulfonic acid immobilized on epichlorohydrin functionalized  $\text{Fe}_3\text{O}_4@/\text{WO}_3$  ( $\text{Fe}_3\text{O}_4@/\text{WO}_3\text{-EAE-SO}_3\text{H}$ ) (III).** To a solution of 2-aminoethanesulfonic acid (5 mmol, 0.7 g) in refluxing NaOH (0.04 M, 30 mL),  $\text{Fe}_3\text{O}_4@/\text{WO}_3\text{-E}$  (II) (0.5 g) was added with stirring under  $\text{N}_2$  atmosphere. After 8 h, the resulting  $\text{Fe}_3\text{O}_4@/\text{WO}_3\text{-EAE-SO}_3\text{H}$  (III) as a dark brown precipitate was separated with a magnet and washed to pH < 7.5 by distilled water and then dried under vacuum at 60 °C overnight.

**2.6 Synthesis of 1-butyl-3-methylimidazolium chloride.** 1-Chlorobutane (10.8 g, 0.8 mol) was added to 1-methylimidazole (8.2 g, 0.1 mol) in a round bottomed flask equipped with a reflux condenser. The mixture was stirred at 70 °C for 48 h. After formation of two phases, the top layer which contains unreacted starting material was decanted. Then ethyl acetate (30 mL) was added with entire mixing followed by its decantation and this step was repeated three times. After the third decanting of ethyl acetate, remaining solvent was removed by heating at 70 °C. The obtained pale yellow liquid was vacuum distilled and the resulting 1-butyl-3-methylimidazolium chloride was placed for vacuum drying at 80 °C in a vacuum drying oven.<sup>68</sup>

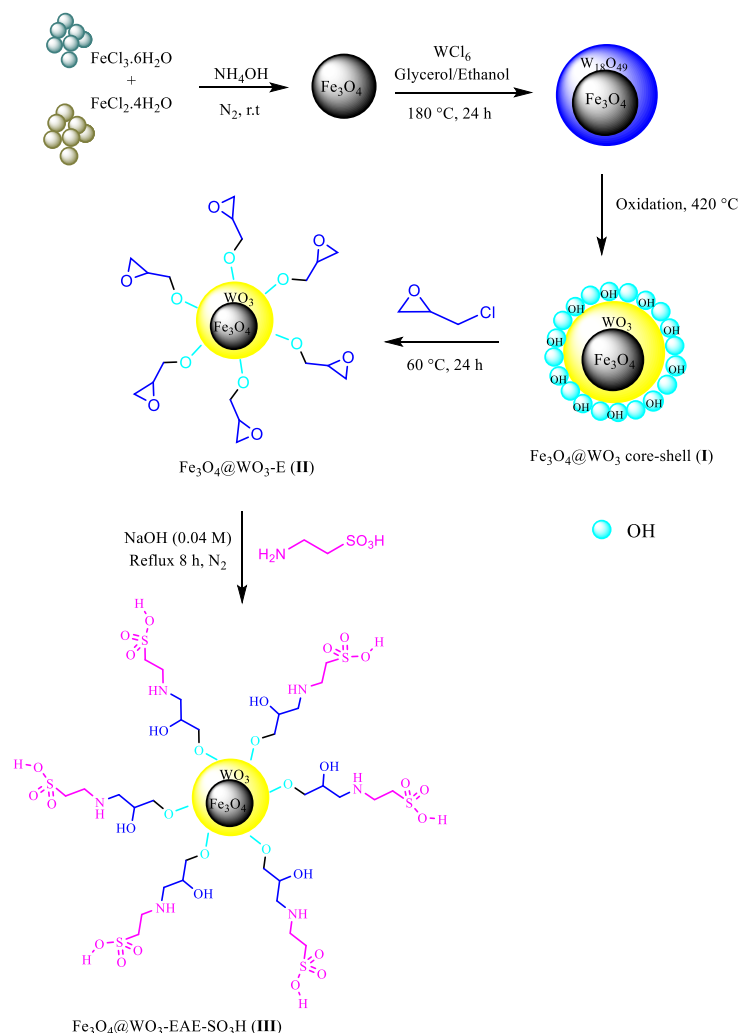
**2.7 Synthesis of 1-butyl-3-methylimidazolium azide.** Freshly prepared 1-butyl-3-methylimidazolium chloride (3.49 g, 20 mmol) and  $\text{NaN}_3$  (1.30 g, 20 mmol) were added into 25 mL deionized water, and the mixture was stirred for 24 h at room temperature. The solvent was removed under reduced pressure at 50 °C. To separate 1-butyl-3-methylimidazolium azide from the crude product (which contains azide ionic liquid and NaCl), the resulting mixture was washed with acetonitrile (3 × 10 mL). The remaining acetonitrile was removed under high vacuum to yield yellow transparent liquid that became more viscous upon extensive drying. Isolated yield was 92% (3.33 g).<sup>69</sup>

**2.8 Typical procedure for synthesis of 1-phenyl-1H-tetrazole in the presence of the  $\text{Fe}_3\text{O}_4@/\text{WO}_3\text{-EAE-SO}_3\text{H}$  (III).**

$\text{Fe}_3\text{O}_4@/\text{WO}_3\text{-EAE-SO}_3\text{H}$  (III) (0.01 g) was added to a solution of aniline (0.093 g, 1.0 mmol), triethyl orthoformate (0.177 g, 1.2 mmol) and 1-butyl-3-methylimidazolium azide (0.216 g, 1.2 mmol) in water (5 mL). The reaction mixture was allowed to stir magnetically at 60 °C for 30 min. After completion of the reaction (as monitored by TLC), the reaction mixture was cooled to room temperature and the catalyst was separated by an external magnet. Then the resulting solution was extracted with EtOAc (3 × 15 mL). The organic layer was washed with brine, dried over anhydrous  $\text{Na}_2\text{SO}_4$  and evaporated under reduced pressure. The crude product was recrystallized from ethylacetate/*n*-hexane (1/9 v/v) to afford the pure 1-phenyl-1H-tetrazole (1.48 g, 95 %). The recovered catalyst was washed with hot ethyl acetate, dried at 60 °C for 2 h and reused for subsequent cycle.

### 3. Results and Discussion

**3.1 Characterization of Catalyst.** The  $\text{Fe}_3\text{O}_4@/\text{WO}_3\text{-EAE-SO}_3\text{H}$  (III) as a magnetically heterogeneous nanocatalyst was prepared according to the pathway shown in Scheme 1. The composition of the newly synthesized nanocatalyst was fully characterized by some technical methods such as Fourier transform infrared (FT-IR) spectroscopy, X-ray diffraction (XRD), transmission electron microscopy (TEM), energy-dispersive X-ray spectroscopy (EDX), thermogravimetric analysis (TGA) field emission scanning electron microscopy (FE-SEM), CHNS and vibrating sample magnetometry (VSM). The obtained results confirmed the successful preparation of the new nanocatalyst. Figure 1 illustrates the FT-IR spectra of (a)  $\text{Fe}_3\text{O}_4$  nanoparticles; (b)  $\text{Fe}_3\text{O}_4@/\text{WO}_3$  core-shell (I); (c) epichlorohydrin functionalized  $\text{Fe}_3\text{O}_4@/\text{WO}_3$  ( $\text{Fe}_3\text{O}_4@/\text{WO}_3\text{-E}$ ) (II) and (d) 2-aminoethanesulfonic acid immobilized on epichlorohydrin functionalized  $\text{Fe}_3\text{O}_4@/\text{WO}_3$  ( $\text{Fe}_3\text{O}_4@/\text{WO}_3\text{-EAE-SO}_3\text{H}$ ) (III). As can be seen, FT-IR spectrum of  $\text{Fe}_3\text{O}_4$  (Figure 1a) showed broad bands at around 650-580  $\text{cm}^{-1}$ , which was attributed to Fe-O vibration. The stretching vibration of W-O bond in  $\text{WO}_3$  was assigned at around 851-770  $\text{cm}^{-1}$  (Figure 1b). Furthermore, the absorption bands at 1619  $\text{cm}^{-1}$  and 3500-3100  $\text{cm}^{-1}$  were attributed to the bending and stretching vibrational modes of the physisorbed water and attached hydroxyl groups on the surface of  $\text{Fe}_3\text{O}_4@/\text{WO}_3$  (I). The epoxy ring which was grafted to the of  $\text{Fe}_3\text{O}_4@/\text{WO}_3$  framework was recognized by the methylene C-H stretching and bending vibration bands at 2872-2920 and 1450  $\text{cm}^{-1}$ , respectively (Figure 1c). An absorption band at 1110  $\text{cm}^{-1}$  was attributed to C-O-C vibrational stretching. These results indicated that the  $\text{Fe}_3\text{O}_4@/\text{WO}_3$  surface has been immobilized by covalent bonded organic epoxy rings. Ring opening of epoxy ring with 2-aminoethanesulfonic acid was asserted by the



**Scheme 1.** Preparation of 2-aminoethanesulfonic acid immobilized on epichlorohydrin functionalized  $\text{Fe}_3\text{O}_4 @ \text{WO}_3$  ( $\text{Fe}_3\text{O}_4 @ \text{WO}_3\text{-EAE-SO}_3\text{H}$  (**III**)).

appearance of absorption bands around  $3402$  and  $1624 \text{ cm}^{-1}$  corresponding to the stretching and bending vibrations of hydroxyl groups, respectively (Figure 1d). Absorption bands at  $1220$  and  $1159 \text{ cm}^{-1}$  related to stretching vibrations of both asymmetric and symmetric modes of S=O bond. Also, the band was depicted at  $1044 \text{ cm}^{-1}$  in the spectrum of  $\text{Fe}_3\text{O}_4 @ \text{WO}_3\text{-EAE-SO}_3\text{H}$  (**III**) related to C–N stretching vibration frequency.

XRD measurement was used to identify the crystalline structure of  $\text{Fe}_3\text{O}_4 @ \text{WO}_3$  MNPs. As shown in Figure 2, the XRD pattern exhibited reflection peaks at  $2\theta = 18.9^\circ, 31.2^\circ, 36.8^\circ, 38.5^\circ, 55.6^\circ$  and  $65.1^\circ$  which can be indexed to (1 1 1), (2 2 0), (3 1 1), (2 2 2), (4 2 2) and (4 4 0) reflections of the cubic structure of  $\text{Fe}_3\text{O}_4$  (JCPDS 19–0629).<sup>70</sup> In addition, diffraction peaks appeared at  $2\theta = 22.7^\circ, 24.0^\circ,$

$33.1^\circ, 34.0^\circ, 41.3^\circ, 52.8^\circ$  and  $61.7^\circ$  corresponding to (0 0 1), (1 1 0), (1 1 1), (2 0 0), (2 0 1), (1 1 2), (2 1 2) and (4 0 0) crystallographic faces, could be assigned to tetragonal structure of  $\text{WO}_3$  (JCPDS 01-085-0807).<sup>71</sup> The average crystallite size,  $d$ , of  $\text{Fe}_3\text{O}_4 @ \text{WO}_3$  MNPs calculated using the Debye–Scherrer equation  $d = K \lambda / \beta \cos \theta$  is about  $15.5 \text{ nm}$ . The morphology and size distribution of  $\text{Fe}_3\text{O}_4 @ \text{WO}_3\text{-EAE-SO}_3\text{H}$  (**III**) was further determined using transmission electron microscopy (TEM), as shown in Figure 3. TEM analysis showed that morphology of the most prepared nanoparticles is spherical in shape and also the size of particles is in the range of  $7\text{--}23 \text{ nm}$ . Moreover, as can be seen the synthesized MNPs have core-shell structure. Furthermore, distribution histogram of  $\text{Fe}_3\text{O}_4 @ \text{WO}_3\text{-EAE-SO}_3\text{H}$  (**III**) revealed that the average diameter of nanoparticles is  $15 \text{ nm}$ , which is in a good agreement with

the results deduced from the XRD. Field emission scanning electron microscopy (FE-SEM) is used to visualize very small topographic details on the surface or fractioned objects. Biology, chemistry and physics applied this technique to observe structures that may be as small as 1 nanometer (= billion of a millimeter). So in order to investigate the surface morphology of  $\text{Fe}_3\text{O}_4@ \text{WO}_3\text{-EAE-SO}_3\text{H}$  (**III**), we used the field emission scanning electron microscopy. FE-SEM images of  $\text{Fe}_3\text{O}_4@ \text{WO}_3\text{-EAE-SO}_3\text{H}$  (**III**) reveals that the nanoparticles have spherical shape with the average particle sizes of about 15-20 nm (Figure 4). The energy dispersive spectrum (EDS) of the catalyst indicates all of the expected elements of  $\text{Fe}_3\text{O}_4@ \text{WO}_3\text{-EAE-SO}_3\text{H}$  (**III**) (C, O, Fe, W and S) as shown in Figure 5. It is clear that 2-aminoethanesulfonic acid was successfully immobilized on epichlorohydrin functionalized  $\text{Fe}_3\text{O}_4@ \text{WO}_3$  ( $\text{Fe}_3\text{O}_4@ \text{WO}_3\text{-E}$ ) (**II**). Also no extra peaks related to any impurity are identified in the nanocatalyst structure. The thermal stability of  $\text{Fe}_3\text{O}_4@ \text{WO}_3\text{-EAE-SO}_3\text{H}$  (**III**) was investigated by thermogravimetric analysis (TGA) (Figure 6). TGA thermogram of  $\text{Fe}_3\text{O}_4@ \text{WO}_3\text{-EAE-SO}_3\text{H}$  (**III**) showed two main weight losses. The first one is related to the adsorbed water molecules on the support

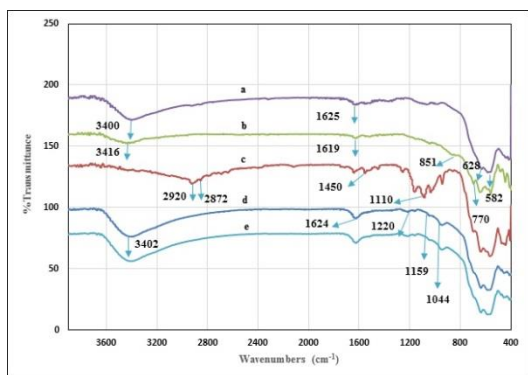


**Figure 1.** FT-IR spectra of (a)  $\text{Fe}_3\text{O}_4$  nanoparticles, (b)  $\text{Fe}_3\text{O}_4@ \text{WO}_3$  core-shell (**I**), (c)  $\text{Fe}_3\text{O}_4@ \text{WO}_3\text{-E}$  (**II**), (d)  $\text{Fe}_3\text{O}_4@ \text{WO}_3\text{-EAE-SO}_3\text{H}$  (**III**), (e) 7th recovered  $\text{Fe}_3\text{O}_4@ \text{WO}_3\text{-EAE-SO}_3\text{H}$  (**III**).

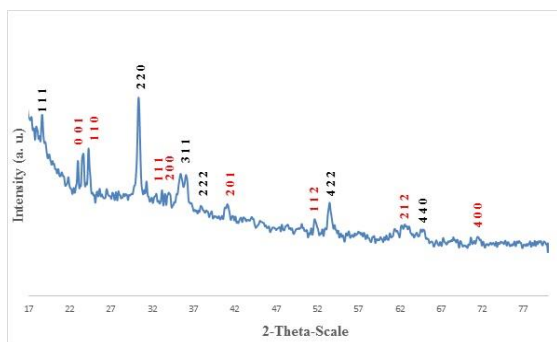


**Figure 2.** XRD pattern of  $\text{Fe}_3\text{O}_4@ \text{WO}_3$  MNPs.

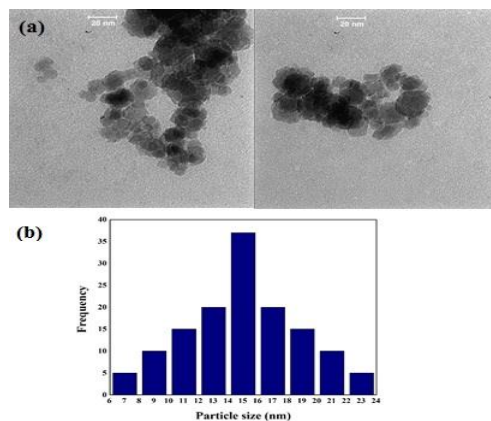


**Figure 3.** (a) TEM of  $\text{Fe}_3\text{O}_4@ \text{WO}_3\text{-EAE-SO}_3\text{H}$  (**III**) and (b) particle size distribution histogram of  $\text{Fe}_3\text{O}_4@ \text{WO}_3\text{-EAE-SO}_3\text{H}$  (**III**).

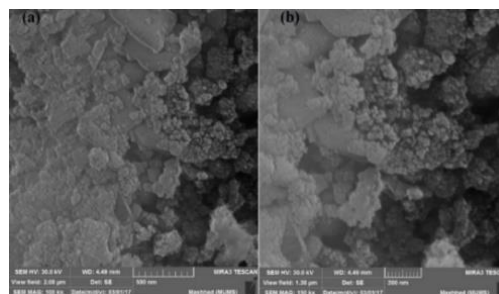


**Figure 4.** The FE-SEM images of  $\text{Fe}_3\text{O}_4@ \text{WO}_3\text{-EAE-SO}_3\text{H}$  (**III**).

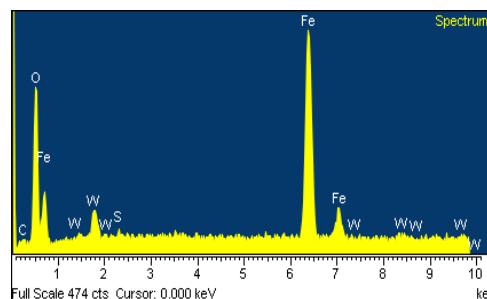


**Figure 5.** The EDS analysis of  $\text{Fe}_3\text{O}_4@ \text{WO}_3\text{-EAE-SO}_3\text{H}$  (**III**).

(weight loss 0.78% at 131–219°C). The second one which occurs at 219–540°C (weight loss 3.49%) is corresponded to the decomposition of organic parts supported on the  $\text{Fe}_3\text{O}_4@ \text{WO}_3$  MNPs surface. According to the TGA, the amount of organic segments supported on  $\text{Fe}_3\text{O}_4@ \text{WO}_3$  MNPs is estimated to be  $0.215 \text{ mmol g}^{-1}$ .

According the elemental analysis data, the loading amount of organic segments supported on  $\text{Fe}_3\text{O}_4@ \text{WO}_3$  (**I**) was  $0.2 \text{ mmol g}^{-1}$  based on carbon, nitrogen and sulfur content (C=1.62%, N=0.31% and S=0.75%). To determine the number of acidic sites in  $\text{Fe}_3\text{O}_4@ \text{WO}_3\text{-EAE-SO}_3\text{H}$

(III), back-titration analysis was performed on the catalyst. The prepared catalyst (100 mg) was suspended in an aqueous NaOH solution (0.1 M, 15 mL), and maintained at room temperature overnight under stirring. Afterwards the suspension was filtered. The filtrate was neutralized by a standard solution of HCl (0.1 M). The amount of loaded -NHCH<sub>2</sub>CH<sub>2</sub>SO<sub>3</sub>H per 1.000 g of Fe<sub>3</sub>O<sub>4</sub>@WO<sub>3</sub>-EAE-SO<sub>3</sub>H (III) was determined by the consumed volume of HCl (14.25 mL) (0.225 mmol of -NHCH<sub>2</sub>CH<sub>2</sub>SO<sub>3</sub>H per 1.000 g of catalyst). This result is in good agreement with those obtained from TGA and elemental analysis. The magnetization curve of Fe<sub>3</sub>O<sub>4</sub>@WO<sub>3</sub>-EAE-SO<sub>3</sub>H (III) was measured at ambient temperature by a vibrating sample magnetometry (VSM). As illustrated in Figure 7, the value of saturation magnetic moments of Fe<sub>3</sub>O<sub>4</sub>@WO<sub>3</sub>-EAE-SO<sub>3</sub>H (III) is Ms= 43.60 emu g<sup>-1</sup> which was lower than the reference value for Fe<sub>3</sub>O<sub>4</sub> particles Ms= 73 emu g<sup>-1</sup>.<sup>72</sup> Decreasing in the saturation magnetization of Fe<sub>3</sub>O<sub>4</sub>@WO<sub>3</sub>-EAE-SO<sub>3</sub>H(III) after surface grafting, can be attributed to the contribution of the non-magnetic materials.

**3.2 Catalytic synthesis of 1-substituted-1H-1,2,3,4-tetrazoles.** As a part of our growing interest in the development of new methods for 5-substituted-1H-tetrazoles synthesis<sup>51,52,54,57,73</sup> and according to the green chemistry legislations, we decided to perform a systematic investigation on the synthesis of 1-substituted-1H-1,2,3,4-tetrazole derivatives under significantly milder conditions using Fe<sub>3</sub>O<sub>4</sub>@WO<sub>3</sub>-EAE-SO<sub>3</sub>H (III) as a new green magnetically separable and efficient heterogeneous nanocatalyst (Scheme 2). Initial experiments were carried out in order to determine the best reaction conditions. Very recently<sup>54,57</sup> we found that using 1-butyl-3-methylimidazolium azide ([bmim][N<sub>3</sub>]) ionic liquid as an azide ion source in place of the highly toxic reagents such as NaN<sub>3</sub> or TMSN<sub>3</sub> predominantly supports the movement toward the green chemistry. Therefore, at the first stage, we probed the optimized reaction conditions including molar ratios of reactants as well as loading of the catalyst, the effect of temperature and solvents in terms of time and yield on the reaction of aniline, triethyl orthoformate and [bmim]N<sub>3</sub> in the presence of Fe<sub>3</sub>O<sub>4</sub>@WO<sub>3</sub>-EAE-SO<sub>3</sub>H (III). The obtained results are summarized in Table 1. For the further understanding of the role of Fe<sub>3</sub>O<sub>4</sub>@WO<sub>3</sub>-EAE-SO<sub>3</sub>H (III) in preparation of 1-phenyl-1H-tetrazole, in a set of experiments the model reaction was conducted in the absence of catalyst as well as in the presence of Fe<sub>3</sub>O<sub>4</sub> NPs, Fe<sub>3</sub>O<sub>4</sub>@WO<sub>3</sub> (I) NPs, and Fe<sub>3</sub>O<sub>4</sub>@WO<sub>3</sub>-E (II) respectively (Table 1, entries 1-4). As it was shown in Table 1, when the reaction was attempted without the addition of catalyst, no desired product was obtained and Fe<sub>3</sub>O<sub>4</sub> NPs, Fe<sub>3</sub>O<sub>4</sub>@WO<sub>3</sub> (I) NPs and Fe<sub>3</sub>O<sub>4</sub>@WO<sub>3</sub>-E (II) provided the target compound with not satisfactory

yields. As proved by control experiments, a considerable increase in the reaction yield was observed using Fe<sub>3</sub>O<sub>4</sub>@WO<sub>3</sub>-EAE-SO<sub>3</sub>H (III) at 110 °C (Table 1, entry 5), while low conversion was obtained when the model reaction was performed at 100 °C (Table 1, entry 6). In an effort to develop better reaction conditions and in continuation of our interest in exploring the utility of green solvents in organic synthesis,<sup>60,64,74</sup> by applying 1:1.2:1 molar ratio of PhNH<sub>2</sub>: HC(OEt)<sub>3</sub>: [bmim]N<sub>3</sub>, the model reaction was carried out in H<sub>2</sub>O at different temperatures (Table 1, entries 7-9). In comparison, in aqueous media the reaction proceeded more efficiently (a reasonable yield of the desired product was obtained at lower temperature) than in solvent free condition. In view of safety, economic and handling considerations, H<sub>2</sub>O was chosen as the best solvent for further experiments. Also, by considering the yield and reaction rate, 60 °C was preferred as the optimal reaction temperature for all of the reactions. Decrease in molar ratio of HC(OEt)<sub>3</sub> reduced the reaction rate obviously, while a further increase in molar ratio of HC(OEt)<sub>3</sub> did not show any further increase in the yield of the product (Table 1, compare entry 10 with entry 12).

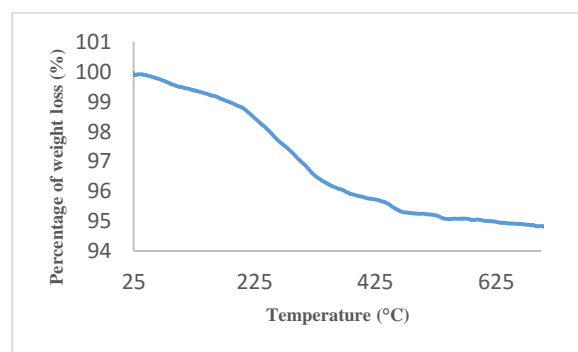


**Figure 6.** TGA thermogram of Fe<sub>3</sub>O<sub>4</sub>@WO<sub>3</sub>-EAE-SO<sub>3</sub>H (III).

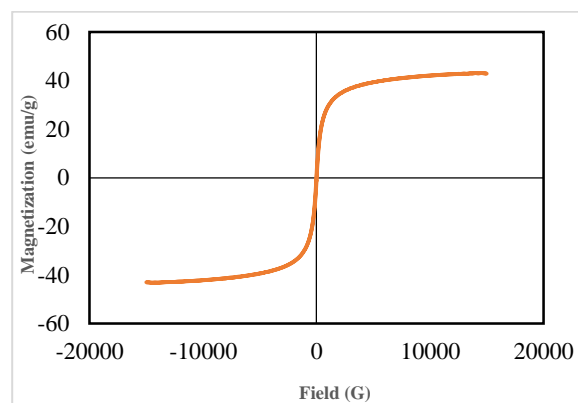
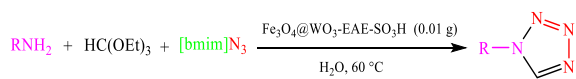


**Figure 7.** Magnetization curve of Fe<sub>3</sub>O<sub>4</sub>@WO<sub>3</sub>-EAE-SO<sub>3</sub>H (III).



R= C<sub>6</sub>H<sub>5</sub>, 4-MeC<sub>6</sub>H<sub>4</sub>, 3,4-Me<sub>2</sub>C<sub>6</sub>H<sub>3</sub>, C<sub>6</sub>H<sub>5</sub>CH<sub>2</sub>, 4-ClC<sub>6</sub>H<sub>4</sub>, 4-BrC<sub>6</sub>H<sub>4</sub>, 4-NO<sub>2</sub>C<sub>6</sub>H<sub>4</sub>, 4-OHC<sub>6</sub>H<sub>4</sub>, 2-OHC<sub>6</sub>H<sub>4</sub>, 2-C<sub>3</sub>H<sub>4</sub>N, 3-MeC<sub>6</sub>H<sub>4</sub>, 3-BrC<sub>6</sub>H<sub>4</sub>, 2-OMe-4-ClC<sub>6</sub>H<sub>3</sub>

**Scheme 2.** Synthesis of different structurally 1-substituted-1*H*-1,2,3,4-tetrazoles using Fe<sub>3</sub>O<sub>4</sub>@WO<sub>3</sub>-EAE-SO<sub>3</sub>H (**III**) in water

However, the increase in molar ratio of [bmim]N<sub>3</sub> up to 1:1.2:1.2 has a profound effect on the yield of the product during the course of reaction (Table 1, compare entry 11 with entry 13). To achieve the optimum amount of the catalyst, the model reaction was investigated at different quantities of Fe<sub>3</sub>O<sub>4</sub>@WO<sub>3</sub>-EAE-SO<sub>3</sub>H (**III**) at 60 °C in H<sub>2</sub>O. The usage of higher amounts of catalyst did not increase the yield significantly, while decreasing the amount of catalyst reduced the yield (Table 1, entries 14-15). To study the efficacy of [bmim]N<sub>3</sub>, when NaN<sub>3</sub> was used as the source of azide ion in the model reaction under the optimized reaction conditions (Table 1, entry 11), the reaction rate was slowed down along with obtaining low yield of product (Table 1, entry 16). To further improve the product yield, the effect of other solvents such as EtOH, PEG, DMF, DMSO, CH<sub>3</sub>CN, 1,4-dioxane and THF have been checked on model reaction. Considering the economic and environmental factors and also based on the results of Table 1, water was chosen as the best solvent for synthesis of 1-substituted-1*H*-1,2,3,4-tetrazoles (Table 1, entry 17-23).

Next, after optimizing the reaction conditions, we attempted to broaden the applicability of the above-described approach using several amines, triethyl orthoformate and [bmim]N<sub>3</sub>. The results are summarized in Table 2. Under similar conditions, it was observed that amines carrying different functional groups (containing electron-withdrawing as well as electron-donating groups) such as methyl, hydroxyl, bromo, chloro and nitro underwent the conversion in short reaction times and in all cases high yields of the desired products were achieved by heating the reaction mixture at 60°C. In comparison the *para*-substituted anilines gave good results than the *ortho*-substituted anilines, because of more steric hindrance for the *ortho*-position anilines on product formation than the *para*-position anilines (entries 6 and 10 *vs.* entry 5 and 9). The present catalytic system also worked well with heterocyclic and aliphatic amines such as 2-amino pyridine and benzylamine to generate the corresponding products with good yields of 95% and 90% respectively (entries 12 and 13). The structural elucidation of the all synthesized 1-substituted-1*H*-1,2,3,4-tetrazoles has been established on the basis of their melting points and mass spectral studies which were in good corroboration with literature and the proposed structures. We have also

reported the <sup>1</sup>H NMR, <sup>13</sup>C NMR and FT-IR spectral data of some selected synthesized 1-substituted-1*H*-1,2,3,4-tetrazoles.

Completion of the reaction was established by the disappearance of amine and formation of desired product on TLC. The Fourier transform infrared (FTIR) spectra of synthesized compounds showed the absence of the –NH<sub>2</sub> absorption bands and appearance a group of bands at around 3150-3007, 833-710 cm<sup>-1</sup> due to stretching and scissoring bending of =C–H, 1691-1596 cm<sup>-1</sup> and 1286–1204 cm<sup>-1</sup> owing to C=N and N=N=N of tetrazole ring respectively. <sup>1</sup>H NMR spectra displayed a singlet resonating signal at around 9.94-8.96 ppm, due to =C–H of the tetrazole ring. In the <sup>13</sup>C NMR spectral study, the signal of the sp<sup>2</sup> hybridized carbon of the tetrazole ring was observed in the expected region around 159-140.4 ppm, which signifies the formation of tetrazole ring. Comprehensive characteristic spectral data for the different synthesized 1-substituted-1*H*-1,2,3,4-tetrazoles have been discussed in the experimental section and "Supporting Information" file.

The reusability of the catalyst is an important property especially for commercial application which it reduces the cost of process. So, to satisfy the green chemistry criteria, the recovery and reusability of Fe<sub>3</sub>O<sub>4</sub>@WO<sub>3</sub>-EAE-SO<sub>3</sub>H (**III**) as a magnetic nanocatalyst was examined on the model reaction under the optimized reaction conditions. After completion of the model reaction, the catalyst was recovered from the reaction mixture simply by a magnetic field. Then the recovered catalyst was washed with hot ethyl acetate, dried at 60 °C for 2 h and reused up to seven more reaction cycles. The results demonstrate that the recycled and reused catalyst showed the same activity as a fresh catalyst and a minimal decrease in yields was observed (the product was obtained in 95%, 95%, 95%, 95%, 95%, 90%, 85% isolated yields after successive cycles). So, the magnetic nanocatalyst can be reused as such without a significant deterioration in catalytic activity (Figure. 8). To ascertain the variation in chemical structure of functional groups and the hydrogen bonding network of the recovered catalyst, the FT-IR spectrum of the 7th recovered Fe<sub>3</sub>O<sub>4</sub>@WO<sub>3</sub>-EAE-SO<sub>3</sub>H (**III**) was recorded (Figure. 1e). It was found that no significant changes were happened in the shape and intensities of the representative absorption bands (Figures 1d *vs.* 1e). Thus, the catalytic system is almost consistent with the fresh catalyst after repeated cycles of the reaction as compared to the fresh catalyst. The activity and selectivity of heterogeneous catalysts may change during the reactions. The activity usually decreases due to either chemical or physical reasons or a combination of both factors. Therefore, a reduction in the activity of Fe<sub>3</sub>O<sub>4</sub>@WO<sub>3</sub>-EAE-SO<sub>3</sub>H (**III**) might be due to the chemisorption of species on catalytic sites which

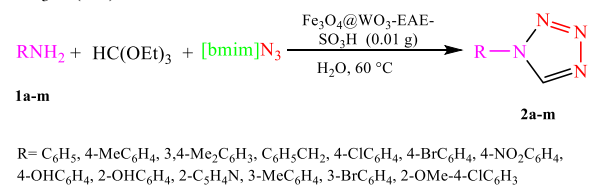
**Table 1.** Optimization of various reaction parameters for the synthesis of 1-phenyl-1*H*-tetrazole in the presence of Fe<sub>3</sub>O<sub>4</sub>@WO<sub>3</sub>-EAE-SO<sub>3</sub>H (**III**).

Entry	Molar ratio of PhNH <sub>2</sub> /HC(OEt) <sub>3</sub> /[bmim]N <sub>3</sub>	Amount of catalyst (g)	Solvent	Temperature (°C)	Time (min)	Isolated Yield (%)
1	1:1.2:1	-	-	110	24 (h)	-
2 <sup>a</sup>	1:1.2:1	0.01	-	110	24 (h)	5
3 <sup>b</sup>	1:1.2:1	0.01	-	110	24 (h)	10
4 <sup>c</sup>	1:1.2:1	0.01	-	110	24 (h)	10
5	1:1.2:1	0.01	-	110	30	95
6	1:1.2:1	0.01	-	100	40	90
7	1:1.2:1	0.01	H <sub>2</sub> O	reflux	25	90
8	1:1.2:1	0.01	H <sub>2</sub> O	60	40	90
9	1:1.2:1	0.01	H <sub>2</sub> O	50	55	85
10	1:1:1	0.01	H <sub>2</sub> O	60	45	80
<b>11</b>	<b>1:1.2:1.2</b>	<b>0.01</b>	<b>H<sub>2</sub>O</b>	<b>60</b>	<b>30</b>	<b>95</b>
12	1:1.5:1.2	0.01	H <sub>2</sub> O	60	30	95
13	1:1.2:1.5	0.01	H <sub>2</sub> O	60	30	95
14	1:1.2:1.2	0.012	H <sub>2</sub> O	60	30	95
15	1:1.2:1.2	0.008	H <sub>2</sub> O	60	55	90
16 <sup>d</sup>	1:1.2:1.2	0.01	H <sub>2</sub> O	60	55	80
17	1:1.2:1.2	0.01	EtOH	60	24 (h)	80
18	1:1.2:1.2	0.01	PEG	60	24 (h)	70
19	1:1.2:1.2	0.01	DMF	60	24 (h)	75
20	1:1.2:1.2	0.01	DMSO	60	24 (h)	40
21	1:1.2:1.2	0.01	CH <sub>3</sub> CN	60	24 (h)	55
22	1:1.2:1.2	0.01	1,4-Dioxane	60	24 (h)	40
23	1:1.2:1.2	0.01	THF	60	24 (h)	30

<sup>a</sup> The reaction was performed in the presence of Fe<sub>3</sub>O<sub>4</sub> NPs. <sup>b</sup> The reaction was performed in the presence of Fe<sub>3</sub>O<sub>4</sub>@WO<sub>3</sub> NPs (**I**).

<sup>c</sup> The reaction was performed in the presence of Fe<sub>3</sub>O<sub>4</sub>@WO<sub>3</sub>-E (**II**). <sup>d</sup> The reaction was performed by using NaN<sub>3</sub>.

**Table 2.** Synthesis of different structurally 1-substituted-1*H*-1,2,3,4-tetrazoles in the presence of Fe<sub>3</sub>O<sub>4</sub>@WO<sub>3</sub>-EAE-SO<sub>3</sub>H (**III**).



Entry	R	Time (min)	Isolated Yield (%)
1	C <sub>6</sub> H <sub>5</sub> <b>1a</b>	30	95
2	4-Me-C <sub>6</sub> H <sub>4</sub> <b>1b</b>	20	95
3	3-Me-C <sub>6</sub> H <sub>4</sub> <b>1c</b>	25	90
4	3,4-Me <sub>2</sub> -C <sub>6</sub> H <sub>3</sub> <b>1d</b>	40	90
5	4-HO-C <sub>6</sub> H <sub>4</sub> <b>1e</b>	25	95
6	2-HO-C <sub>6</sub> H <sub>4</sub> <b>1f</b>	60	95
7	4-Br-C <sub>6</sub> H <sub>4</sub> <b>1g</b>	35	90
8	3-Br-C <sub>6</sub> H <sub>4</sub> <b>1h</b>	55	90
9	4-Cl-C <sub>6</sub> H <sub>4</sub> <b>1i</b>	40	90
10	2-OMe-4-Cl-C <sub>6</sub> H <sub>3</sub> <b>1j</b>	95	90
11	4-NO <sub>2</sub> -C <sub>6</sub> H <sub>4</sub> <b>1k</b>	50	90
12	2-C <sub>5</sub> H <sub>4</sub> N <b>1l</b>	35	95
13	C <sub>6</sub> H <sub>5</sub> CH <sub>2</sub> <b>1m</b>	45	90

blocks the sites of nanocatalyst. Also the deactivation of catalyst might be caused by the physical deposit of reactants onto the catalyst surface or in the catalyst pores.<sup>86</sup>

In subsequent experiments, to show the superiority of Fe<sub>3</sub>O<sub>4</sub>@WO<sub>3</sub>-EAE-SO<sub>3</sub>H (**III**) over a variety of the reported catalysts in the literature, a comparative study was conducted on model reaction (Table 3). As shown in Table 3 (entries 1-5 and entries 8-9), the model reaction in the presence of In(OTf)<sub>3</sub>, natrolite zeolite, SSA, Cu

NPs/bentonite, ZnS nanoparticles and HClO<sub>4</sub>-SiO<sub>2</sub>, was completed at higher temperature (100-120 °C) by taking prolonged time period as well (50-360 min). However, nano ZnS/US and immobilized AlCl<sub>3</sub> on Al<sub>2</sub>O<sub>3</sub> afforded the desired product quickly at lower temperature but by using DMF as solvent (Table 3, entries 6-7). Quick route to 1-phenyl-1*H*-tetrazole was obtained using [Hbm]BF<sub>4</sub>, Fe<sub>3</sub>O<sub>4</sub>@SiO<sub>2</sub>/Salen Cu(II) and Fe<sub>3</sub>O<sub>4</sub>@silica sulfonic acid as catalyst but at higher temperature (Table 3, entries 10-12). It is clear that Fe<sub>3</sub>O<sub>4</sub>@WO<sub>3</sub>-EAE-SO<sub>3</sub>H (**III**) worked remarkably well, as the desired product was produced at 60 °C within 30 min in H<sub>2</sub>O along with easy separation using an external magnet. Then Fe<sub>3</sub>O<sub>4</sub>@WO<sub>3</sub>-EAE-SO<sub>3</sub>H (**III**) can be the catalyst of choice for the present synthetic method.

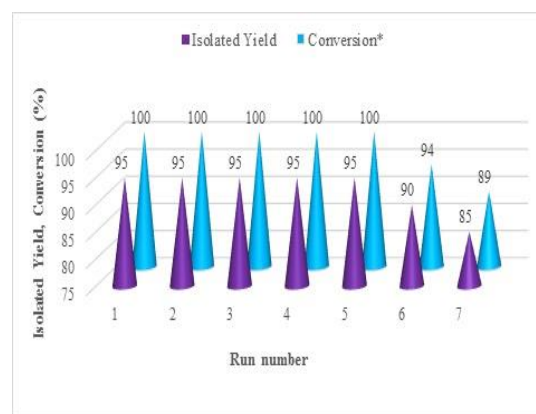


**Figure 8.** Synthesis of 1-phenyl-1*H*-tetrazole in the presence of reused Fe<sub>3</sub>O<sub>4</sub>@WO<sub>3</sub>-EAE-SO<sub>3</sub>H (**III**).

#### 4. Conclusion

In summary, a convenient, eco-friendly and scalable approach for the synthesis of 1-substituted-1*H*-1,2,3,4-tetrazoles using Fe<sub>3</sub>O<sub>4</sub>@WO<sub>3</sub>-EAE-SO<sub>3</sub>H (**III**) as a catalyst was reported. Fe<sub>3</sub>O<sub>4</sub>@WO<sub>3</sub>-EAE-SO<sub>3</sub>H (**III**) as a novel heterogeneous nanocatalyst was prepared and characterized by FT-IR, XRD, TEM, FE-SEM, EDS, TGA, CHNS and VSM techniques. Characterization results validate that magnetic nanocatalyst Fe<sub>3</sub>O<sub>4</sub>@WO<sub>3</sub>-EAE-SO<sub>3</sub>H (**III**) with spherical shape and mean diameters of 7–23 nm was successfully synthesized. Subsequently, the new synthesized nanocatalyst has been used for the synthesis of structurally different 1-substituted-1*H*-1,2,3,4-tetrazoles via the cyclization reaction of various primary amines, triethyl orthoformate and 1-butyl-3-methylimidazolium azide ([bmim][N<sub>3</sub>]) under benign reaction conditions.

The noteworthy features of this green synthetic protocol are enhanced reaction rate, mild reaction conditions, operational simplicity, excellent yield, high purity, clean reaction profile, using magnetic separation technique and the potential reusability of the catalyst. Moreover, the present synthetic method eliminates the use of harmful

solvents and hazardous materials thus provides a better scope for the synthesis of 1-substituted-1*H*-1,2,3,4-tetrazoles. This notable and valuable feature of this methodology makes it a more helpful and practical alternative to the other existing methods for synthesizing this class of compounds in organic chemistry and also in medicinal chemistry.

The authors gratefully acknowledge the partial support of this study by Ferdowsi University of Mashhad Research Council (Grant no. p/3/43366).

#### Supporting Information

The Supporting Information contains characterization data of all compounds. This material is available on <http://dx.doi.org/>

**Table 3** Comparison between efficiency of Fe<sub>3</sub>O<sub>4</sub>@WO<sub>3</sub>-EAE-SO<sub>3</sub>H (**III**) and some other catalysts for the synthesis of 1-phenyl-1*H*-tetrazole.

Entry	Catalyst	Solvent	Temperature (°C)	Time (min)	Yield (%)	Ref.
1	In(OTf) <sub>3</sub>	-	100	120	90	75
2	Natrolite zeolite	-	120	240	94	76
3*	SSA	-	120	300	95	77
4	Cu NPs/bentonite	-	120	180	93	78
5	Yb(OTf) <sub>3</sub>	CH <sub>3</sub> OC <sub>2</sub> H <sub>4</sub> OH	100	360	85	30
6	Nano ZnS/U.S	DMF	r.t	20	92	79
7	Immobilized AlCl <sub>3</sub> on Al <sub>2</sub> O <sub>3</sub>	DMF	50	60	94	80
8	ZnS nanoparticles	-	130	270	78	81
9	HClO <sub>4</sub> -SiO <sub>2</sub>	-	120	240	89	82
10	[Hbim]BF <sub>4</sub>	-	100	25	89	83
11	Fe <sub>3</sub> O <sub>4</sub> @SiO <sub>2</sub> /Salen Cu(II)	-	100	60	96	84
12	Fe <sub>3</sub> O <sub>4</sub> @silica sulfonic acid	-	100	50	97	85
13	Fe <sub>3</sub> O <sub>4</sub> @WO <sub>3</sub> -EAE-SO <sub>3</sub> H ( <b>III</b> )	H <sub>2</sub> O	60	30	95	Present study

\* Silica Sulfuric Acid.

#### References

1 B. Jawabrah Al-Hourani, W. Al-Awaida, K. Z. Matalka, M. I. El-Barghouthi, F. Alsoubani, F. Wuest, *Bioorg. Med. Chem. Lett.* **2016**, *26*, 4757.

2 L. B. Moskvina, A. V. Bulatov, G. L. Griogorjev, G. I. Koldobskii, *J. Flow Injection Anal.* **2003**, *20*, 53-58.

3 A. Burger, *Prog. Drug Res.* **1991**, *37*, 287.

4 A. R. Modarresi-Alam, F. Khamooshi, M. Rostamizadeh, H. Keykha, M. Nasrollahzadeh, H. R. Bijanzadeh, E. Kleinpeter, *J. Mol. Struct.* **2007**, *841*, 61.

5 F. Ek, L. G. Wistrand, T. Frejd, *Tetrahedron* **2003**, *59*, 6759.

6 L. A. Flippin, *Tetrahedron Lett.* **1991**, *32*, 6857.

7 P. Rhonnstad, D. Wensbo, *Tetrahedron Lett.* **2002**, *43*, 3137.

8 R. E. Ford, P. Knowles, E. Lunt, S. M. Marshall, A. J. Penrose, C. A. Ramsden, A. J. H. Summers, J. L. Walker, D. E. Wright, *J. Med. Chem.* **1986**, *29*, 538.

9 N. P. Peet, L. E. Baugh, S. Sundler, J. E. Lewis, E. H. Matthews, E. L. Olberding, D. N. Shah, *J. Med. Chem.* **1986**, *29*, 2403.

10 V. V. Nikulin, T. V. Artamonova, G. I. Koldobskii, *Russ. J. Org. Chem.* **2003**, *39*, 1525.

11 V. V. Nikulin, T. V. Artamonova, G. I. Koldobskii, *Russ. J. Org. Chem.* **2005**, *41*, 444.

- 12 L. V. Myznikov, A. Hrabalek, G. I. Koldobskii, *Chem. Heterocycl. Compd.* **2007**, *43*, 1.
- 13 R. N. Butler, A. R. Katritzky, C. W. Rees, E. F. V. Scriven, *Comprehensive Heterocyclic Chemistry II*, Pergamon Oxford **1996**, *4*, 621.
- 14 H. Singh, A. S. Chawla, V. K. Kapoor, D. Paul, R. K. Malhotra, *Prog. Med. Chem.* **1980**, *17*, 151.
- 15 V. A. Ostrovskii, M. S. Pevzner, T. P. Kofmna, M. B. Sheherbinin, I. V. Tselinskii, *Targets Heterocycl. Syst.* **1999**, *3*, 467.
- 16 M. Hiskey, D. E. Chavez, D. L. Naud, S. F. Son, H. L. Berghout, C. A. Bome, *Proc. Int. Pyrotech. Semin.* **2000**, *27*, 3.
- 17 M. J. Genin, D. A. Allwine, D. J. Anderson, M. R. Barbachyn, D. E. Emmert, S. A. Garmon, D. R. Graber, K. C. Grega, J. S. Hester, D. K. Hutchinson, J. Morris, R. J. Reischer, C. W. Ford, G. E. Zurenko, J. C. Hamel, R. D. Schaadt, D. Stapert, B. H. Yagi, *J. Med. Chem.* **2000**, *43*, 953.
- 18 R. N. Butler, *Adv. Heterocycl. Chem.* **1977**, *21*, 323.
- 19 F.R. Benson, *Chem. Rev.* **1947**, *47*, 1.
- 20 P. K. Kadaba, *Synthesis* **1973**, 71.
- 21 S. J. Wittenberger, *Org. Prep. Proced. Int.* **1994**, *26*, 499.
- 22 A. R. Katritzky, B. V. Rogovoy, K. V. Kovalenko, *J. Org. Chem.* **2003**, *68*, 4941.
- 23 M. L. Kantam, K. B. S. Kumar, K. P. Raja, *J. Mol. Catal. A: Chem.* **2006**, *247*, 186.
- 24 R. J. Herr, *Bioorg. Med. Chem.* **2002**, *10*, 3379.
- 25 D. M. Zimmerman, R. A. Olofson, *Tetrahedron Lett.* **1969**, *10*, 5081.
- 26 T. Jin, S. Kamijo, Y. Yamamoto, *Tetrahedron Lett.* **2004**, *45*, 9435.
- 27 F. G. Fallon, R. M. Herbst, *J. Org. Chem.* **1957**, *22*, 933.
- 28 Y. Satoh, N. Marcopulos, *Tetrahedron Lett.* **1995**, *36*, 1759.
- 29 A. K. Gupta, C. H. Oh, *Tetrahedron Lett.* **2004**, *45*, 4113.
- 30 W. Su, Z. Hong, W. Shan, X. Zhang, *Eur. J. Org. Chem.* **2006**, 2723.
- 31 S. N. Dighe, K. S. Jain, K. V. Srinivasan, *Tetrahedron Lett.* **2009**, *50*, 6139.
- 32 S. V. Voitekhovich, A. N. Vorob'ev, P. N. Gaponik, O. A. Ivashkevich, *Chem. Heterocycl. Compd.* **2005**, *41*, 999.
- 33 A. K. Gupta, C. Y. Rim, C. H. Oh, *Synlett* **2004**, 2227.
- 34 A. K. Gupta, C. H. Song, C. H. Oh, *Tetrahedron Lett.* **2004**, *45*, 4113.
- 35 N. T. Pokhodylo, V. S. Matiychuk, M. D. Obushak, *Tetrahedron* **2008**, *64*, 1430.
- 36 a) T. Zeng, W. W. Chen, C. M. Cirtiu, A. Moores, G. Song, C. J. Li, *Green Chem.* **2010**, *12*, 570, b) V. Polshettiwar, R. Luque, A. Fihri, H. Zhu, M. Bouhrara, J. M. Basset, *Chem. Rev.* **2011**, *111*, 3036, c) D. Wang, D. Astruc, *Chem. Rev.* **2014**, *114*, 6949, d) C. W. Lim, I. S. Lee, *Nano Today* **2010**, *5*, 412, e) M. B. Gawande, P. S. Branco, R. S. Varma, *Chem. Soc. Rev.* **2013**, *42*, 3371.
- 37 A. Ali, H. Zafar, M. Zia, I. ul Haq, A. R. Phull, J. S. Ali, A. Hussain, *Nanotechnol. Sci. Appl.* **2016**, *9*, 49.
- 38 B. Liu, W. Zhang, F. Yang, H. Feng, X. Yang, *J. Phys. Chem. C* **2011**, *115*, 15875.
- 39 Y. S. Li, J. S. Church, A. L. Woodhead, F. Moussa, *Spectrochim. Acta Mol. Biomol. Spectrosc.* **2010**, *76*, 484.
- 40 Y. Deng, C. Deng, D. Qi, C. Liu, J. Liu, X. Zhang, D. Zhao, *Adv. Mater.* **2009**, *21*, 1377.
- 41 Y. Dong, M. Hu, R. Ma, H. Cheng, S. Yang, Y. Y. Li, J. A. Zapien, *CrystEngComm* **2013**, *15*, 1324.
- 42 W. Xie, X. Zang, *Food Chem.* **2017**, *227*, 397.
- 43 Y. Li, X. Xu, D. Qi, C. Deng, P. Yang, X. Zhang, *J. Proteome Res.* **2008**, *7*, 2526.
- 44 A. Amoozadeh, S. Rahmani, *J. Mol. Catal. A: Chem.* **2015**, *396*, 96.
- 45 H. Zheng, J. Z. Ou, M. S. Strano, R. B. Kaner, A. Mitchell, K. Kalantar-zadeh, *Adv. Funct. Mater.* **2011**, *21*, 2175.
- 46 K. Suzuki, T. Watanabe, S. I. Murahashi, *J. Org. Chem.* **2013**, *78*, 2301.
- 47 D. H. Koo, M. Kim, S. Chang, *Org. Lett.* **2005**, *7*, 5015.
- 48 S. S. Enumula, V. R. B. Gurram, R. R. Chada, D. R. Burri, S. R. R. Kamaraju, *J. Mol. Catal. A: Chem.* **2017**, *426*, 30.
- 49 M. Amini, A. Yousefi, *Reac. Kinet. Mech. Cat.* **2016**, *119*, 207.
- 50 G. Xi, B. Yue, J. Cao, J. Ye, *Chem. Eur. J.* **2011**, *17*, 5145.
- 51 N. Razavi, B. Akhlaghinia, *RSC Adv.* **2015**, *5*, 12372.
- 52 S. S. E. Ghodsinia, B. Akhlaghinia, *RSC Adv.* **2015**, *5*, 49849.
- 53 M. Zarghani, B. Akhlaghinia, *Appl. Organomet. Chem.* **2015**, *29*, 683.
- 54 R. Jahanshahi, B. Akhlaghinia, *RSC Adv.* **2015**, *5*, 104087.
- 55 N. Y. Siavashi, B. Akhlaghinia, M. Zarghani, *Res. Chem. Intermed.* **2016**, *42*, 5789.
- 56 R. Jahanshahi, B. Akhlaghinia, *RSC Adv.* **2016**, *6*, 29210.
- 57 M. Zarghani, B. Akhlaghinia, *RSC Adv.* **2016**, *6*, 31850.
- 58 M. Zarghani, B. Akhlaghinia, *RSC Adv.* **2016**, *6*, 38592.
- 59 S. M. Masjed, B. Akhlaghinia, M. Zarghani, N. Razavi, *Aust. J. Chem.* **2017**, *70*, 33.
- 60 S. S. E. Ghodsinia, B. Akhlaghinia, R. Jahanshahi, *RSC Adv.* **2016**, *6*, 63613.
- 61 M. Zarghani, B. Akhlaghinia, *Bull. Chem. Soc. Jpn.* **2016**, *89*, 1192.
- 62 Z. Zarei, B. Akhlaghinia, *RSC Adv.* **2016**, *6*, 106473.
- 63 N. Razavi, B. Akhlaghinia, R. Jahanshahi, *Catal. Lett.* **2017**, *147*, 360.
- 64 N. Razavi, B. Akhlaghinia, *New J. Chem.* **2016**, *40*, 447.
- 65 S. Sobhani, M. S. Ghasemzadeh, M. Honarmand, F. Zarifi, *RSC Adv.* **2014**, *4*, 44166.
- 66 H. Ripps, W. Shen, *Mol. Vis.* **2012**, *18*, 2673.
- 67 F. Shirini, N. Daneshvar, *RSC Adv.* **2016**, *6*, 110190.
- 68 P. N. Tshibangu, S. N. Ndwandwe, E. D. Dikio, *Int. J. Electrochem. Sci.* **2011**, *6*, 2201.

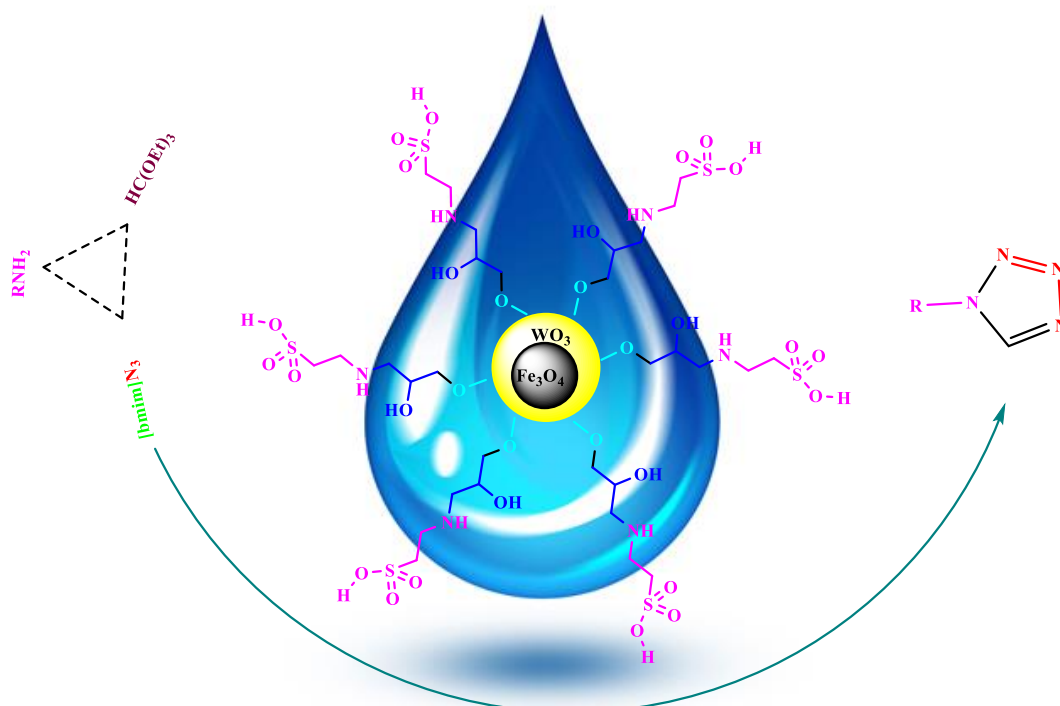
- 69 H. Valizadeh, M. Amiri, E. Khalili, *Mol. Diversity* **2012**, *16*, 319.
- 70 M. Esmaeilpour, A. R. Sardarian, J. Javidi, *Appl Catal A: Gen* **2012**, *445–446*, 359.
- 71 W. L. Kehl, R. G. Hay, D. Wahl, *J. Appl. Phys.* **1952**, *23*, 212.
- 72 S. Li, H. Bai, J. Wang, X. Jing, Q. Liu, M. Zhang, R. Chen, L. Liu, C. Jiao, *Chem. Eng. J.* **2012**, *193–194*, 372.
- 73 B. Akhlaghinia, S. Rezazadeh, *J. Braz. Chem. Soc.* **2012**, *23*, 2197.
- 74 S. Rezazadeh, B. Akhlaghinia, E. K. Goharshadi, H. Sarvari, *J. Chin. Chem. Soc.* **2014**, *61*, 1108.
- 75 D. Kundu, A. Majee, A. Hajra, *Tetrahedron Lett.* **2009**, *50*, 2668.
- 76 D. Habibi, M. Nasrollahzadeh, T. A. Kamali, *Green Chem.* **2011**, *13*, 3499.
- 77 D. Habibi, H. Nabavi, M. Nasrollahzadeh, *J. Chem.* **2013**, *4*.
- 78 A. Rostami-Vartooni, M. Alizadeh, M. Bagherzadeh, *Beilstein. J. Nanotechnol.* **2015**, *6*, 2300.
- 79 H. Naeimi, F. Kiani, *Ultrason. Sonochem.* **2015**, *27*, 408.
- 80 H. M. Nanjundaswamy, H. Abrahamse, *Heterocycles* **2014**, *89*, 2137.
- 81 H. Naeimi, F. Kiani, M. Moradian, *J. Nanopart. Res.* **2014**, *16*, 2590.
- 82 S. Bahari, A. Rezaei, *Lett. Org. Chem.* **2014**, *11*, 55.
- 83 T. M. Potewar, S. A. Siddiqui, R. J. Lahoti, K. V. Srinivasan, *Tetrahedron Lett.* **2007**, *48*, 1721.
- 84 F. Dehghani, A. R. Sardarian, M. Esmaeilpour, *J. Organomet. Chem.* **2013**, *743*, 87.
- 85 H. Naeimi, S. Mohamadabadi, *Dalton Trans.* **2014**, *43*, 12967.
- 86 M. D. Argyle, C. H. Bartholomew, *Catalysts* **2015**, *5*, 145.

## Graphical Abstract

**2-Aminoethanesulfonic acid immobilized on epichlorohydrin functionalized  $\text{Fe}_3\text{O}_4@ \text{WO}_3$  ( $\text{Fe}_3\text{O}_4@ \text{WO}_3\text{-EAE-SO}_3\text{H}$ ): a novel magnetically recyclable heterogeneous nanocatalyst for the green one-pot synthesis of 1-substituted-1*H*-1,2,3,4-tetrazoles in water**

Maryam Sadat Ghasemzadeh and Batool Akhlaghinia\*

A novel method for preparing 1-substituted-1*H*-1,2,3,4-tetrazoles with high yield of products using  $\text{Fe}_3\text{O}_4@ \text{WO}_3\text{-EAE-SO}_3\text{H}$  (**III**) as a magnetic nanocatalyst, was investigated. This new methodology is cost-effective and offers several advantages such as excellent yields of products, mild reaction conditions, minimization of chemical waste, broad substrate scope, simple work-up procedure and magnetic separation of the nanocatalyst, make this protocol very attractive for the synthesis of a variety of 1-substituted-1*H*-1,2,3,4-tetrazoles.



$\text{R} = \text{C}_6\text{H}_5, 4\text{-MeC}_6\text{H}_4, 3,4\text{-Me}_2\text{C}_6\text{H}_3, \text{C}_6\text{H}_5\text{CH}_2, 4\text{-ClC}_6\text{H}_4, 4\text{-BrC}_6\text{H}_4, 4\text{-NO}_2\text{C}_6\text{H}_4, 4\text{-OHC}_6\text{H}_4, 2\text{-OHC}_6\text{H}_4, 2\text{-C}_5\text{H}_4\text{N}, 3\text{-MeC}_6\text{H}_4, 3\text{-BrC}_6\text{H}_4, 2\text{-OMe-4-ClC}_6\text{H}_3.$